THE ROLE OF TEXTURE DEVELOPMENT AND DISLOCATIONS IN ACOUSTOELASTICITY DURING PLANE DEFORMATION

George C. Johnson, T. E. Wong, and S. E. Chen

Department of Mechanical Engineering
University of California, Berkeley
Berkeley, CA 94720

INTRODUCTION

Acoustoelasticity is a technique of nondestructive evaluation which relates changes in the stress state acting on a body to changes in the speeds at which waves propagate through the body. The nature of the acoustoelastic effect is well understood under elastic deformations and has been studied under plastic deformations of a polycrystalline aggregate [1-4]. While several phenomenological theories [5-7] have been proposed to describe the effect of plasticity on the acoustoelastic response, the roles of the various microstructural mechanisms which contribute to this effect have not been clearly identified. The purpose of the present work is to examine the effects of two specific mechanisms: the reorientation of grains which accompanies plastic deformation and the motion of dislocations under the applied forces.

Our work consists of analysis of the grain reorientation, or texture development, through use of the Taylor theory [8] and of experiments which show the contribution of dislocations in a polycrystalline aggregate of high purity copper. We begin with a brief outline of the Taylor theory, then review the previous work involving the effects of dislocations on the ultrasonic wave speed. Taylor theory predictions of velocity changes caused by texture development are then compared with measurements for a rolled plate of 5086-H32 aluminum subjected to small plastic deformations (less than 3% plastic strain). Finally, experimental observations of the velocity changes which occur during elastic deformations of the copper sample are presented and discussed.

MODELS FOR THE EFFECTS OF MICROSTRUCTURE ON VELOCITY

In this section we introduce the basic theories which allow the evaluation of the velocity changes caused by texture development and dislocation activity. While our ultimate goal is to obtain a quantitative description of the effect of each mechanism, we recognize that our present experimental observations are not sufficiently complete to permit this. Thus, we will be somewhat more qualitative and ask the questions: what are the essential characteristics of each effect, and can the existing theories give predictions of velocity changes which are of the order of those observed?

Effect of Texture Development

The Taylor theory [8] provides a method for evaluating the texture development (reorientation of crystallites) which accompanies the plastic deformation of a polycrystalline aggregate. It is based on the assumption that plastic deformation within a crystallite is the result of dislocation motion on certain discrete slip systems. Further, it is assumed that each grain of an aggregate is subjected to the same macroscopic strain as the aggregate itself. Since slip occurs only on discrete systems, the macroscopic plastic strain is achieved through several such systems becoming active (slipping) at once. The usual approach is to require that the plastic strain be isochoric so that, in general, at least five independent slip systems must become active. The selection of which particular combination of slips occurs is based on the assumption that the correct combination will minimize the plastic work done.

The Taylor theory for the evaluation of texture development is usually applied to problems in which the plastic strains are large (greater than 25%). In this work, we consider the crystallographic reorientation which occurs under the application of small plastic strains (less than 3%). Because we are dealing with such small deformations, and because we are interested in demonstrating the effect on acoustoelasticity in a somewhat qualitative sense, we have used the simplest version of the Taylor theory.

In this theory, we introduce right-handed Cartesian coordinate systems x_i and x_i^* with unit base vectors $\underset{\sim}{e}_i$ and $\underset{\sim}{e}_i^*$ which are aligned with the principal symmetry axes of the sample and of a particular crystal, respectively. Within this crystal, we assume that there are N discrete slip systems for which unit vectors $\underset{\sim}{b}^{(k)}$ and $\underset{\sim}{n}^{(k)}$, k=1,2,...,N, identify the slip direction and the normal to the slip plane, respectively.

In considering the deformation of the crystal, we distinguish between the slips on the various active slip systems, each of which leaves the crystal basis $\underset{\sim}{e}_i^*$ unaltered, and the rotation of $\underset{\sim}{e}_i^*$ associated with the crystal's reorientation. Treating this in a manner similar to the polar decomposition of the deformation gradient, we consider that the slip occurs first and is followed by the rotation. We thus write

$$\underset{\sim}{F} = \underset{\sim}{r}\,\underset{\sim}{s} \tag{1}$$

where $\underset{\sim}{F}$ is the deformation gradient, $\underset{\sim}{r}$ is the proper orthogonal tensor associated with the rotation of $\underset{\sim}{e}_i^*$, and $\underset{\sim}{s}$ is the deformation gradient associated with slip alone. If only one slip system were active, say the k-th system, the slip tensor $\underset{\sim}{s}$ could be written as

$$\underset{\sim}{s} = \underset{\sim}{I} + s^{(k)}\,\underset{\sim}{b}^{(k)} \otimes \underset{\sim}{n}^{(k)} \tag{2}$$

where $\underset{\sim}{I}$ is the identity tensor and $s^{(k)}$ is the shear on this system. As discussed above, though, more than one slip system will generally become active. We again treat this deformation as a series of slips on individual systems, and so write

$$\underset{\sim}{s} = (\underset{\sim}{I} + s^{(N)}\underset{\sim}{b}^{(N)}\otimes\underset{\sim}{n}^{(N)}) \ldots (\underset{\sim}{I} + s^{(2)}\underset{\sim}{b}^{(2)}\otimes\underset{\sim}{n}^{(2)})(\underset{\sim}{I} + s^{(1)}\underset{\sim}{b}^{(1)}\otimes\underset{\sim}{n}^{(1)}). \tag{3}$$

Noting that the $s^{(k)}$ are small (we typically take steps of less than 0.5% total plastic strain), Eq.(3) can be linerized in $s^{(k)}$ as

$$\underset{\sim}{s} = \underset{\sim}{I} + \sum_{k=1}^{N} s^{(k)}\,\underset{\sim}{b}^{(k)} \otimes \underset{\sim}{n}^{(k)}. \tag{4}$$

Let us now introduce the Lagrange strain $\underset{\sim}{E}$ as

$$\underset{\sim}{E} = (\underset{\sim}{F}^T\underset{\sim}{F} - \underset{\sim}{I})/2 = (\underset{\sim}{s}^T\underset{\sim}{s} - \underset{\sim}{I})/2 \tag{5}$$

where the second of Eq.(5) results from the orthogonality of $\underset{\sim}{r}$. Using Eq. (4) in (5) gives

$$\underset{\sim}{E} = \sum_{k=1}^{N} s^{(k)}[\underset{\sim}{b}^{(k)} \otimes \underset{\sim}{n}^{(k)} + \underset{\sim}{n}^{(k)} \otimes \underset{\sim}{b}^{(k)}]/2 \ . \tag{6}$$

Since $\underset{\sim}{F}$, and so $\underset{\sim}{E}$, are assumed to be given, Eq.(6) can be use to compute the $s^{(k)}$ for each combination of 5 of the N slip systems. The combination of slip systems which achieves the strain $\underset{\sim}{E}$ with the least plastic work is then taken to be the combination which leads to $\underset{\sim}{s}$. Given $\underset{\sim}{s}$, Eq.(1) can be solved for $\underset{\sim}{r}$ as

$$\underset{\sim}{r} = \underset{\sim}{F}\ \underset{\sim}{s}^{-1} \ . \tag{7}$$

We assume in this work that slip occurs only on systems of the type {111}<110> and that there is no hardening present. When the 12 slip systems of this type are taken in sets of 5 for the calculation of $\underset{\sim}{s}$, it is found that often several different sets have the same minimum plastic work. In such cases, $\underset{\sim}{s}$ is taken to be the mean of the various tensors associated with the minimum work. The rotation $\underset{\sim}{r}$ is then calculated from this mean $\underset{\sim}{s}$.

Our calculation of the changes in acoustoelastic response which result from the texture development is based on the work in [9]. In that work, the orientation matrix t_{ij}, which relates the crystal coordinates to the sample coordinates as

$$x_i^* = t_{ij}\, x_j \tag{8}$$

is the primary quantity of interest in evaluating the SOEC and TOEC of the aggregate. The elements t_{ij} are actually the components relative to $\underset{\sim}{e}_i^*$ of a two-point tensor $\underset{\sim}{t}$ which relates the base vectors as

$$\underset{\sim}{e}_i = \underset{\sim}{t}\ \underset{\sim}{e}_i^* \ . \tag{9}$$

Since $\underset{\sim}{r}$ rotates the original crystal basis $\underset{\sim}{e}_i^*$ into a new basis, say $\underset{\sim}{e}_i'$, as

$$\underset{\sim}{e}_i' = \underset{\sim}{r}\ \underset{\sim}{e}_i^* \ . \tag{10}$$

the transformation tensor $\underset{\sim}{t}'$ which relates the new $\underset{\sim}{e}_i'$ to the unchanged $\underset{\sim}{e}_i$ is

$$\underset{\sim}{t}' = \underset{\sim}{t}\ \underset{\sim}{r}^T \ . \tag{11}$$

Effect of Dislocations

It has been well documented that in certain high purity materials, the effect of dislocation motion on ultrasonic velocity can be substantial. Hikata et al. [10,11] examined the velocity and attenuation of longitudinal and shear waves propagating along the axis of aluminum samples subjected to plastic deformation in uniaxial tension. They concluded that the vibrating string model of dislocation interaction with the acoustic waves (Granato and Lücke [12]) gives predictions which are in excellent agreement with their observations. This relatively simple model treats the dislocation loops as strings under tension with effective mass and damping. Two key features of this model are: 1) the introduction of the natural frequencies of the dislocation loop which are inversely proporsional to the loop length and 2) the relation between these natural frequencies and the frequency of the ultrasonic wave. The vibrating string model indicates that the ultrasonic velocity should decrease relative to the velocity in a perfect crystal and that the maximum decrease should occur when the ultrasonic frequency is near

the fundamental natural frequency of the dislocation loops. Further, for fixed loop length and ultrasonic frequency, the decrease should be proportional to the dislocation density.

The experiments of Hikata et al. [10,11] involved deformations into the plastic range so that the dislocations experienced permanent slip. Other work [13-15] has shown that dislocations can have a substantial effect on velocity change during loading even when the applied forces are not of sufficient magnitude to cause plastic deformation. Alers [13] measured the velocity change of longitudinal waves propagating along the loading direction of a copper single-crystal under uniaxial compression. The measurements were made on the crystal in two different conditions. In one condition, the crystal had been annealed so that the dislocation loops were long and the associated fundamental frequency was low. In the other condition, the same crystal had been subjected to γ-ray irradiation, thus having much shorter dislocation loops caused by the increase in pinning points (vacancies created by the radiation). For sufficiently small stresses, the velocity changes caused by the loading were reversible in both cases, but the magnitude of the change was nearly 50 times greater in the annealed material than in the irradiated material. Alers concluded that "even though the dislocations may not break away from pinning points to produce irreversible plastic flow, they still vibrate and modify the sound velocity".

An analytical explanation of this phenomenon is given by Suzuki et al. [14] through an extension of the Granato-Lücke theory which accounts for the bowing of dislocations prior to their unpinning under the application of a static external stress. It is shown that the increase in loop length due to bowing can have an appreciable influence on the ultrasonic velocity even before macroscopic plastic strain occurs.

One particularly interesting aspect of both theories for the dislocation effects [12,14] is that the expected change in velocity caused by external loading should be independent of the sign of the loading. In this work we consider uniaxial tension and compression. Since the action of the applied stress on the dislocation is through the resolved shear stress on the appropriate slip system, the amount of change in loop length which results should be the same in either loading case. Thus, we would expect that changes in velocity caused by dislocation motion should be the same, both in magnitude and sign, in tension and compression. Measurements of the acoustoelastic response of polycrystalline copper (Fukuoka and Toda [15] and this work) support this expectation.

EXPERIMENTAL CONSIDERATIONS

Measurements of two types are reported in this paper. First, x-ray diffraction pole figures are required in evaluating the initial orientation distribution function (ODF) of the aluminum before applying the Taylor theory analysis. Second, measurements of velocity change during applied tension or compression are required in characterizing the acoustoelastic response of the aluminum and copper.

A series of four incomplete pole figures is used in evaluating the ODF. For each pole figure, soft x-rays from a copper source impinge on a flat sample at the Bragg angle associated with the {222}, {220}, {200} or {311} plane of interest. The x-ray intensity is measured in the reflection mode to construct the pole figures [16]. The calculation of the ODF is then obtained through an "inversion" of the incomplete pole figures according to the scheme of Humbert and Bunge [17].

Ultrasonic measurements were made using the double-pulse echo system

described by Ilić et al. [18]. This system operates in a phase-locked loop in which the RF carrier frequency of the ultrasonic wave is varied as the wave's travel time changes so that a specific phase condition is maintained. The measured frequency change is then the change in "natural velocity" introduced by Thurston and Brugger [19], and is related to the change in actual velocity through the change in path length.

In cases when plastic deformations are involved, this change in path length is obtained through use of strain gages. We have found, however, that the specific geometry of the samples used for the measurement of acoustoelastic response during plastic deformations requires a correction to the measured strain in order to obtain an accurate estimate of thickness change. These samples have a gage section where the ultrasonic and strain measurements are made which has an initially rectangular cross-section of 10 mm by 15 mm and which is 14.3 mm long. This relatively short gage section is required in order to ensure that yielding occur within the region of observation. Unfortunately, it is not sufficiently long to allow a fully uniaxial stress state to develop. As a result the cross-section after plastic deformation is no longer rectangular, but is either cupped in (tension) or barreled out (compression) on the sides. The extent of this effect has been characterized using a surface roughness measuring instrument and has been shown to be repeatable from sample to sample. The data in this paper which involve elastic-plastic deformations take this effect into account. Similar data given in [3] did not take this effect into account.

The materials involved in this study are the 5086-H32 aluminum described in [3] and a plate of OFHC copper (ASTM specification F 68) nominally 19.1 mm (3/4 in.) thick. The copper is at least 99.99% pure and is in the half-hard condition with a macroscopic yield stress of around 200 MPa. Measurements of changes in the actual velocities of longitudinal and shear waves in the aluminum during elastic-plastic deformations and of changes in the natural velocities in the copper during elastic deformations are reported.

RESULTS

The ODF has been calculated from the four pole figure measurements made on the 5086-H32 aluminum. Pole figures for {222} and {200} planes are shown in Figs. 1a and b. Reconstructions of the complete pole figures from the calculated ODF are shown in Figs. 1c and d for the {222} and {200} planes.

A hypothetical aggregate consisting of 431 grains with orientations chosen so as to reproduce the ODF obtained from the x-ray analysis was generated for application of the Taylor theory. The velocities of pure mode waves propagating in the principal directions of anisotropy were computed for the original aggregate through a Voigt averaging of the stiffness [9]. The macroscopic strain associated with uniaxial tension along either the rolling direction or transverse direction was then imposed on each grain and the resulting shears and rotations were calculated. Finally, the velocities were computed for the deformed aggregate and the velocity change per unit plastic strain was evaluated.

Figures 2, 3 and 4 show the experimental data (solid lines) and predictions (dashed lines) for velocity change of the three pure mode waves propagating in the plate's normal direction for tension along the rolling direction, compression along the rolling direction, and tension along the transverse direction, respectively. In each case the loading consisted of cycles of uniaxial loading which took the material through the elastic range into the plastic range then followed by complete unloading. The predicted velocity change is given only at zero stress (completely unloaded material) and so should be compared to the end of the unloading cycles. As in [3] we

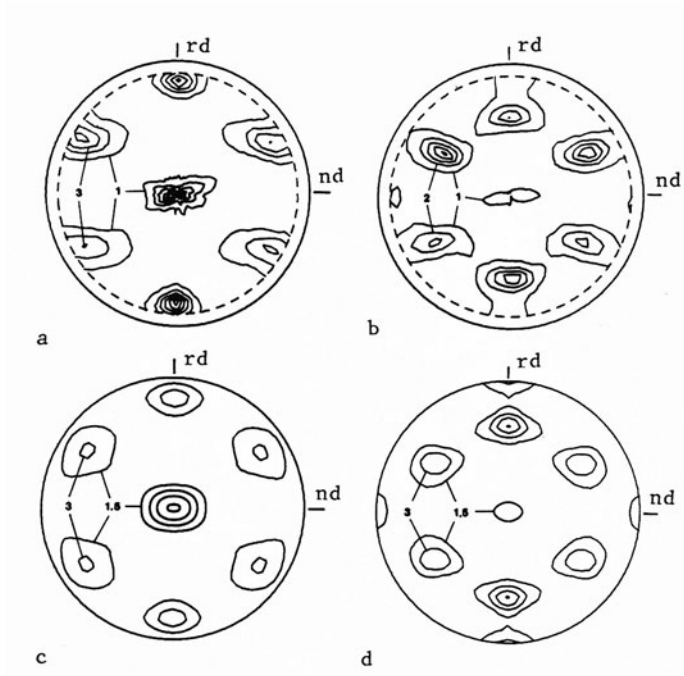

Fig. 1 Pole figures for 5086-H32 aluminum. (a) Experimental {222}, (b) experimental {200}, (c) reconstructed {222}, (d) reconstructed {200}. Values given are multiples of random distribution.

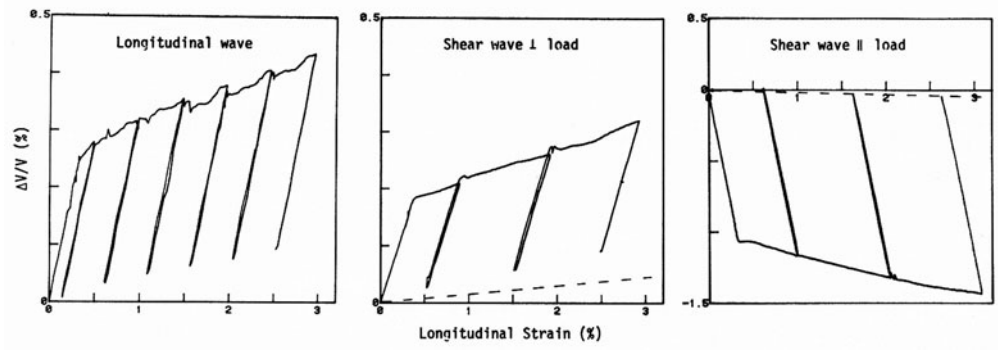

Fig. 2 Relative velocity change versus longitudinal strain for 5086-H32 during uniaxial tension along the rolling direction. Wave propagation is in the normal direction.

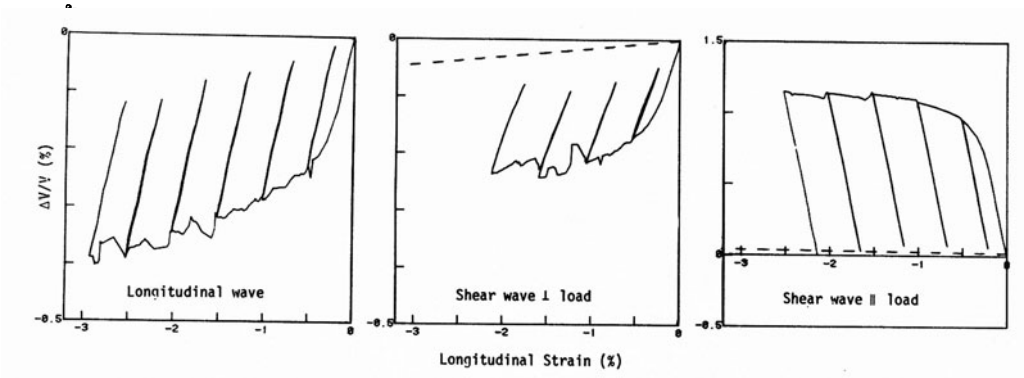

Fig. 3 Relative velocity change versus longitudinal strain for 5086-H32 during uniaxial compression along the rolling direction. Wave propagation is in the normal direction.

TABLE I. Comparison of predicted versus observed changes in velocity with plastic deformation for 5086-H32 aluminum.

Loading Direction	Loading Type	Data Type[a]	Contraction Ratio	ΔV/V per Unit Plastic Strain		
				Longitudinal	Shear ⊥ Load	Shear ∥ Load
Rolling	Tension	E	0.59	0.041	0.037	-0.01
Rolling	Compression	E	0.74	0.047	0.049	-0.02
Rolling	Either	P	0.64	-0.0008	0.015	-0.012
Transverse	Tension	E	0.45	0.023	0.038	-0.045
Transverse	Either	P	0.40	0.002	0.0045	-0.013

[a] E = Experimental; P = Predicted

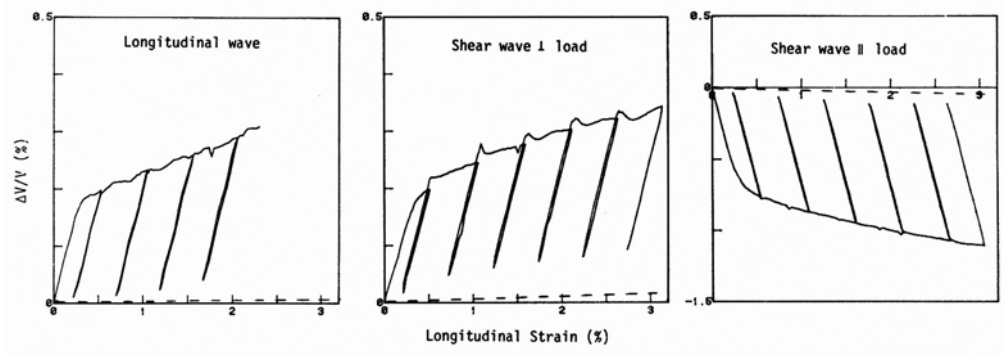

Fig. 4 Relative velocity change versus longitudinal strain for 5086-H32 during uniaxial tension along the transverse direction. Wave propagation is in the normal direction.

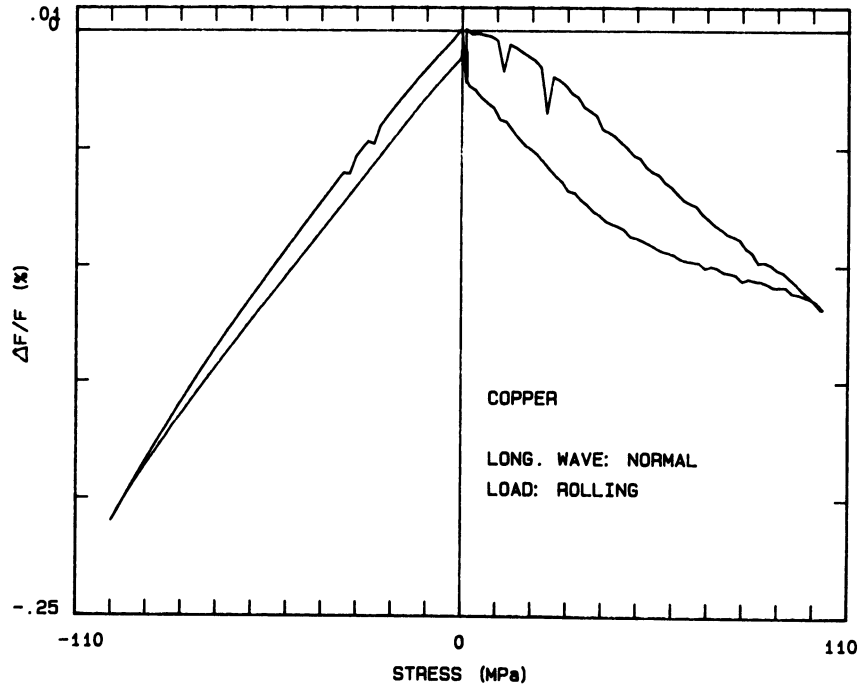

Fig. 5 Relative frequency (natural velocity) change versus uniaxial stress in OFHC copper for longitudinal waves.

represent the change in velocity per unit plastic strain through the slope of the line which best fits the velocity change at zero stress. A listing of the observed and predicted changes in velocity per unit plastic strain is given in Table I.

An examination of Table I shows that the development of texture provides a reasonable explanation for the observed changes in shear wave speed, but not for the observed changes in longitudinal wave speed. For the shear waves, the predicted changes are of the correct sign and order of magnitude, but tend to be slightly smaller than the observed changes. The Taylor theory predictions indicate that the longitudinal wave speeds should not change. As noted in [3], the fact that the sign of the change in velocity depends upon the sign of the loading indicates that these changes are not caused by changes in the dislocation state.

We now turn our attention to the OFHC copper. Figure 5 shows the change in natural velocity for longitudinal waves propagating in the normal direction versus uniaxial stress along the rolling direction. Figure 6 shows similar curves for shear waves propagating in the normal direction and polarized in the transverse direction. This data shows that the wave speeds decrease during elastic deformations in both tension and compression. Thus, as noted in [15], this data is inconsistent with the usual acoustoelastic theory. It is, however, consistent with the dislocation theory of Suzuki, et al. [14].

Since no macroscopic plastic deformation took place in the copper, no change in texture took place. Thus, the observed changes in wave speed in the copper are dominated by the dislocation activity. The separation of the two effects is not as clear, however, for the aluminum. The results of Allison et al. [4] suggest that this separation might be at least partially obtained by continuing the tests beyond the point of complete unloading to examine the acoustoelastic response (or stress-acoustic constant) in both tension and compression. Their work shows that small plastic strains can lead to a deviation in the values of the stress-acoustic constant measured in

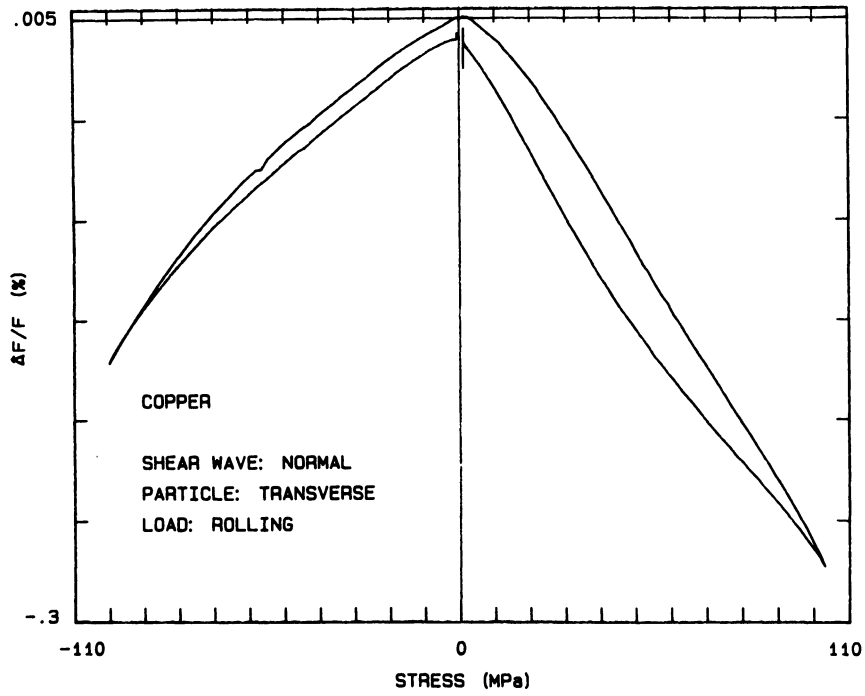

Fig. 6 Relative frequency (natural velocity) change vs. uniaxial stress in OFHC copper for shear waves polarized perpendicular to the loading.

tension and compression. Their deviation is similar, though not nearly as extreme, as that seen in the copper results.

ACKNOWLEDGEMENTS

This work is supported by the National Science Foundation under grant No. MEA 8410535. We are grateful to Professor H. R. Wenk of the Department of Geology and Geophysics for making his x-ray diffraction equipment available for this work and for many useful discussions on quantitative texture analysis.

REFERENCES

1. G. C. Johnson, J. Appl. Mech. 48, 791 (1981).
2. M. Hirao and Y. H. Pao, J. Acoust. Soc. Am. 77, 1659 (1985).
3. T. E. Wong and G. C. Johnson, The Acoustoelastic Response of an Aluminum Plate During Elastic-Plastic Deformation, in "Review of Progress in Quantitative NDE, Vol. 5," D. O. Thompson and D. E. Chimenti, ed., Plenum Press, New York (1986).
4. S. G. Allison, J. S. Heyman and K. Salama, Ultrasonic Characterization of Plastic Deformation in Metals, in "Review of Progress in Quantitative NDE, Vol. 5," D. O. Thompson and D. E. Chimenti, ed., Plenum Press, New York (1986).
5. G. C. Johnson, J. Acoust. Soc. Am. 70, 591 (1981).
6. M. Kobayashi, Trans. JSME A48, 432 (1982).
7. G. C. Johnson, J. Appl. Mech. 50, 689 (1983).
8. G. I. Taylor, J. Inst. Metals 62, 307 (1938).
9. G. C. Johnson, J. Appl. Mech. 52, 659 (1985).
10. A. Hikata, R. Truell, A. Granato, B. Chick and K. Lücke, J. Appl. Phys. 27, 396 (1956).
11. A. Hikata, B. Chick, C. Elbaum and R. Truell, Acta Met. 10, 423 (1962).
12. A. V. Granato and K Lücke, J. Appl. Phys. 27, 583 (1956).

13. G. Alers, The Measurement of Very Small Sound Velocity Changes and Their Use in the Study of Solids, in "Physical Acoustics, Vol. 4a," W. P. Mason, ed., Academic Press, New York (1966).
14. T. Suzuki, A. Hikata and C. Elbaum, J. Appl. Phys. 35, 2761 (1964).
15. H. Fukuoka and H. Toda, Arch. Mech. 29, 673 (1977).
16. H. R. Wenk, Measurement of Pole Figures, in "Preferred Orientation in Deformed Metals and Rocks: An Introduction to Modern Texture Analysis," H. R. Wenk, ed., Academic Press, Orlando, FL (1985).
17. M. Humbert and H. J. Bunge, Incomplte Pole Figure Method, in: "Quantitative Texture Analysis," H. J. Bunge and C. Esling, ed., Deutsche Gesellschaft fur Metallkunde, Oberursel (1982).
18. D. B. Ilić, G. S. Kino and A. R. Selfridge, Rev. Sci. Instrum. 50, 1527 (1979).
19. R. N. Thurston and K. Brugger, Phys. Rev. 133, A1604 (1964).